

Robust nodal superconductivity induced by isovalent doping in $\text{Ba}(\text{Fe}_{1-x}\text{Ru}_x)_2\text{As}_2$ and $\text{BaFe}_2(\text{As}_{1-x}\text{P}_x)_2$

X. Qiu,¹ S. Y. Zhou,¹ H. Zhang,¹ B. Y. Pan,¹ X. C. Hong,¹ Y. F. Dai,¹
 Man Jin Eom,² Jun Sung Kim,² Z. R. Ye,¹ Y. Zhang,¹ D. L. Feng,¹ S. Y. Li^{1,*}

¹*Department of Physics, State Key Laboratory of Surface Physics,
 and Laboratory of Advanced Materials, Fudan University, Shanghai 200433, China*

²*Department of Physics, Pohang University of Science and Technology, Pohang 790-784, Korea*

(Dated: August 19, 2021)

We present the ultra-low-temperature heat transport study of iron-based superconductors $\text{Ba}(\text{Fe}_{1-x}\text{Ru}_x)_2\text{As}_2$ and $\text{BaFe}_2(\text{As}_{1-x}\text{P}_x)_2$. For optimally doped $\text{Ba}(\text{Fe}_{0.64}\text{Ru}_{0.36})_2\text{As}_2$, a large residual linear term κ_0/T at zero field and a \sqrt{H} dependence of $\kappa_0(H)/T$ are observed, which provide strong evidences for nodes in the superconducting gap. This result demonstrates that the isovalent Ru doping can also induce nodal superconductivity, as P does in $\text{BaFe}_2(\text{As}_{0.67}\text{P}_{0.33})_2$. Furthermore, in underdoped $\text{Ba}(\text{Fe}_{0.77}\text{Ru}_{0.23})_2\text{As}_2$ and heavily underdoped $\text{BaFe}_2(\text{As}_{0.82}\text{P}_{0.18})_2$, κ_0/T manifests similar nodal behavior, which shows the robustness of nodal superconductivity in the underdoped regime and puts constraint on theoretical models.

PACS numbers: 74.70.Xa, 74.25.fc, 74.20.Rp

Since the discovery of high- T_c superconductivity in iron pnictides [1, 2], the electronic pairing mechanism has been a central issue [3]. One key to understand it is to clarify the symmetry and structure of the superconducting gap [4]. However, even for the most studied $(\text{Ba}, \text{Sr}, \text{Ca}, \text{Eu})\text{Fe}_2\text{As}_2$ (122) system, the situation is still fairly complex [4].

Near optimal doping, for both hole- and electron-doped 122 compounds, the angle-resolved photon emission spectroscopy (ARPES) experiments clearly demonstrated multiple nodeless superconducting gaps [5, 6], which was further supported by bulk measurements such as thermal conductivity [7–9]. On the overdoped side, nodal superconductivity was found in the extremely hole-doped KFe_2As_2 [10, 11], while strongly anisotropic gap [9], or isotropic gaps with significantly different magnitudes [12, 13] were suggested in the heavily electron-doped $\text{Ba}(\text{Fe}_{1-x}\text{Co}_x)_2\text{As}_2$. On the underdoped side, recent heat transport measurements claimed possible nodes in the superconducting gap of hole-doped $\text{Ba}_{1-x}\text{K}_x\text{Fe}_2\text{As}_2$ with $x < 0.16$ [14], in contrast to the nodeless gaps found in electron-doped $\text{Ba}(\text{Fe}_{1-x}\text{Co}_x)_2\text{As}_2$ [9].

Intriguingly, nodal superconductivity was also found in optimally doped $\text{BaFe}_2(\text{As}_{0.67}\text{P}_{0.33})_2$ ($T_c = 30$ K) [15, 16], in which the superconductivity is induced by isovalent P doping. The ARPES experiments have given conflicting results on the position of the nodes [17, 18]. Moreover, previously LaFePO ($T_c \sim 6$ K) displays clear nodal behavior [19–21], and recently there is penetration depth evidence for nodes in the superconducting gap of LiFeP ($T_c \sim 4.5$ K) [22]. The nodal superconductivity in these P-doped compounds are very striking, which raises the puzzling question why the P doping is so special in iron-based superconductors. The theoretical explanations of this puzzle are far from consensus [23–26].

A recent proposal is that the nodal state in iron-

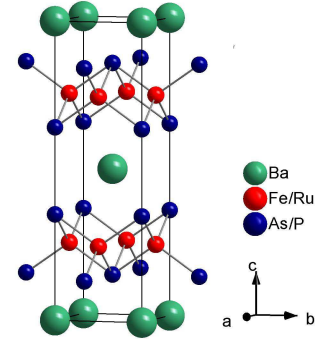


FIG. 1: (Color online). Isovalent doping in the Fe_2As_2 slabs of BaFe_2As_2 , by substituting As with P, or Fe with Ru. Both ways can induce superconductivity, and result in similar phase diagrams.

pnictide superconductors, except for KFe_2As_2 , is induced when the pnictogen height h_{Pn} from the iron plane decreases below a threshold value of ~ 1.33 Å [22]. According to this proposal, there may exist a transition from nodal to nodeless state tuned by h_{Pn} , for example, in underdoped $\text{BaFe}_2(\text{As}_{1-x}\text{P}_x)_2$. Therefore, it is important to investigate the doping evolution of the superconducting gap structure in $\text{BaFe}_2(\text{As}_{1-x}\text{P}_x)_2$. In another aspect, since isovalent substituting Fe with Ru in BaFe_2As_2 , as shown in Fig. 1, can also decrease h_{Pn} and result in similar phase diagram [27–29], it will be very interesting to check whether the gap of $\text{Ba}(\text{Fe}_{1-x}\text{Ru}_x)_2\text{As}_2$ has nodes.

In this Letter, we report the demonstration of nodal superconductivity in optimally doped $\text{Ba}(\text{Fe}_{0.64}\text{Ru}_{0.36})_2\text{As}_2$, underdoped $\text{Ba}(\text{Fe}_{0.77}\text{Ru}_{0.23})_2\text{As}_2$, and heavily underdoped $\text{BaFe}_2(\text{As}_{0.82}\text{P}_{0.18})_2$ by thermal conductivity measurements down to 50 mK. Our finding of nodal gap in

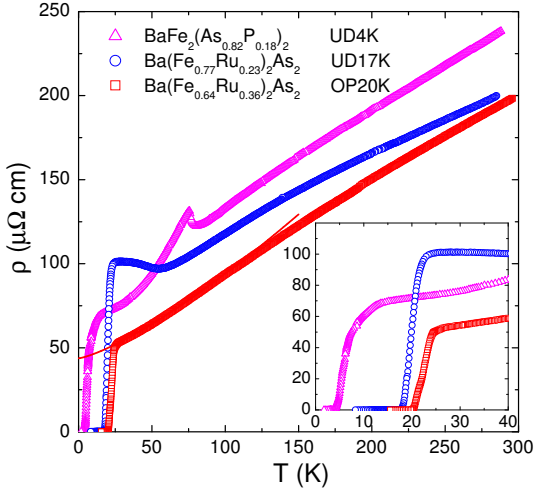


FIG. 2: (Color online). In-plane resistivity of $\text{Ba}(\text{Fe}_{0.64}\text{Ru}_{0.36})_2\text{As}_2$, $\text{Ba}(\text{Fe}_{0.77}\text{Ru}_{0.23})_2\text{As}_2$, and $\text{BaFe}_2(\text{As}_{0.82}\text{P}_{0.18})_2$ single crystals. The low-temperature superconducting transitions are shown in the inset. Defined by $\rho = 0$, the transition temperatures $T_c = 20$, 17, and 4 K are obtained, therefore these three samples are named as OP20K, UD17K, and UD4K, respectively. The solid line is a fit of the data between 30 and 90 K to $\rho(T) = \rho_0 + AT^n$ for the OP20K sample.

$\text{Ba}(\text{Fe}_{0.64}\text{Ru}_{0.36})_2\text{As}_2$ suggests a common origin of the nodal superconductivity induced by isovalent P and Ru doping. The nodal gap in $\text{Ba}(\text{Fe}_{0.77}\text{Ru}_{0.23})_2\text{As}_2$ and $\text{BaFe}_2(\text{As}_{0.82}\text{P}_{0.18})_2$ shows no transition from nodal to nodeless state in the underdoped regime.

Single crystals of $\text{Ba}(\text{Fe}_{1-x}\text{Ru}_x)_2\text{As}_2$ and $\text{BaFe}_2(\text{As}_{1-x}\text{P}_x)_2$ were grown according to the methods described in Refs. [30, 31]. The Ru and P doping levels were determined by energy dispersive X-ray spectroscopy. The sample was cleaved to a rectangular shape with typical dimensions $\sim 1.50 \times 0.7 \text{ mm}^2$ in the ab -plane, and 40 to 80 μm in c -axis. In-plane thermal conductivity was measured in a dilution refrigerator, using a standard four-wire steady-state method with two RuO_2 chip thermometers, calibrated *in situ* against a reference RuO_2 thermometer. Magnetic fields were applied along the c -axis. To ensure a homogeneous field distribution in the samples, all fields were applied at temperature above T_c .

Fig. 2 shows the in-plane resistivity $\rho(T)$ of $\text{Ba}(\text{Fe}_{0.64}\text{Ru}_{0.36})_2\text{As}_2$, $\text{Ba}(\text{Fe}_{0.77}\text{Ru}_{0.23})_2\text{As}_2$, and $\text{BaFe}_2(\text{As}_{0.82}\text{P}_{0.18})_2$ single crystals. The transition temperatures defined by $\rho = 0$ are $T_c = 20$, 17, and 4 K, therefore we name these three samples as OP20K, UD17K, and UD4K, respectively. One can see clear resistivity anomalies in UD4K and UD17K, but not in OP20K, which manifest the gradual suppression of spin-density-wave (SDW) order upon P or Ru doping [28, 29, 32]. For OP20K, the resistivity data between 30 and 90 K are fitted to $\rho(T) = \rho_0 + AT^n$, which gives a

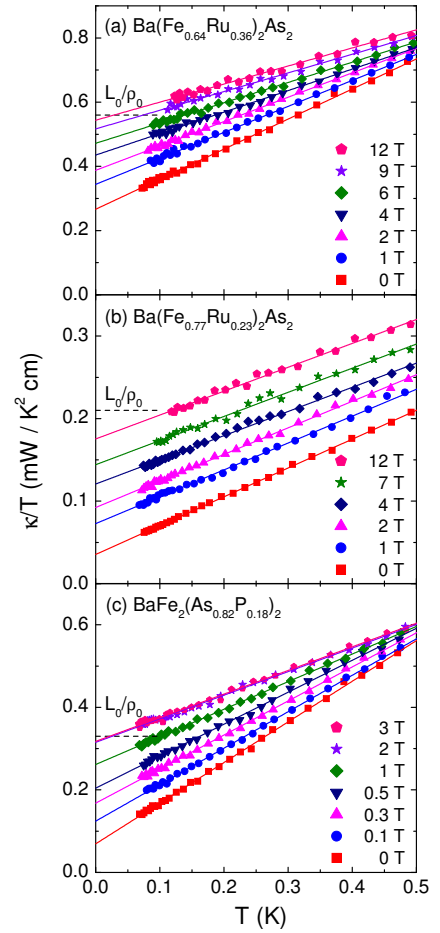


FIG. 3: (Color online). Low-temperature in-plane thermal conductivity of $\text{Ba}(\text{Fe}_{0.64}\text{Ru}_{0.36})_2\text{As}_2$, $\text{Ba}(\text{Fe}_{0.77}\text{Ru}_{0.23})_2\text{As}_2$, and $\text{BaFe}_2(\text{As}_{0.82}\text{P}_{0.18})_2$ in zero and magnetic fields applied along the c -axis. The solid lines are $\kappa/T = a + bT$ fit to all the curves, respectively. The dash lines are the normal-state Wiedemann-Franz law expectation L_0/ρ_0 , with L_0 the Lorenz number $2.45 \times 10^{-8} \text{ W}\Omega\text{K}^{-2}$ and normal-state $\rho_0 = 44$, 115, and 74 $\mu\Omega\text{cm}$, respectively.

residual resistivity $\rho_0 = 43.7 \pm 0.1 \mu\Omega\text{cm}$ and $n = 1.31 \pm 0.1$. Such a non-Fermi-liquid temperature dependence of $\rho(T)$ is similar to that observed in $\text{BaFe}_2(\text{As}_{1-x}\text{P}_x)_2$ near optimal doping, which may reflect the presence of anti-ferromagnetic spin fluctuations near a quantum critical point [32].

The resistivity of these samples were also measured in magnetic fields, the highest up to 14.5 T, in order to determine their upper critical field H_{c2} and normal-state ρ_0 . For OP20K, UD17K, and UD4K, we estimate $H_{c2} = 23$, 19, and 5 T, and normal-state $\rho_0 = 44$, 115, and 74 $\mu\Omega\text{cm}$, respectively.

Fig. 3 shows the temperature dependence of the in-plane thermal conductivity for OP20K, UD17K, and UD4K in zero and magnetic fields, plotted as κ/T vs T . All the curves are roughly linear, as previously observed in $\text{BaFe}_{1.9}\text{Ni}_{0.1}\text{As}_2$ [8], KFe_2As_2 [10], and over-

doped $\text{Ba}(\text{Fe}_{1-x}\text{Co}_x)_2\text{As}_2$ single crystals [9, 12]. Therefore we fit all the curves to $\kappa/T = a + bT^{\alpha-1}$ with α fixed to 2. The two terms aT and bT^α represent contributions from electrons and phonons, respectively. Here we only focus on the electronic term.

For OP20K in zero field, the fitting gives a residual linear term $\kappa_0/T = 0.266 \pm 0.002 \text{ mW K}^{-2} \text{ cm}^{-1}$. This value is more than 40% of the normal-state Wiedemann-Franz law expectation $\kappa_{N0}/T = L_0/\rho_0 = 0.56 \text{ mW K}^{-2} \text{ cm}^{-1}$, with L_0 the Lorenz number $2.45 \times 10^{-8} \text{ W}\Omega\text{K}^{-2}$ and normal-state $\rho_0 = 44 \mu\Omega\text{cm}$. For optimally doped $\text{BaFe}_2(\text{As}_{0.67}\text{P}_{0.33})_2$ single crystal, similar value of $\kappa_0/T \approx 0.25 \text{ mW K}^{-2} \text{ cm}^{-1}$ was obtained, which is about 30% of its normal-state κ_{N0}/T [16]. The significant κ_0/T of $\text{Ba}(\text{Fe}_{0.64}\text{Ru}_{0.36})_2\text{As}_2$ in zero field is attributed to nodal quasiparticles, which is a strong evidence for nodes in the superconducting gap [33].

With decreasing doping level, for UD17K and UD4K, $\kappa_0/T = 35 \pm 1$ and $69 \pm 1 \mu\text{W K}^{-2} \text{ cm}^{-1}$ are obtained, as seen in Figs. 3(b) and 3(c). These values are about 17% and 22% of their normal-state κ_{N0}/T , respectively. We note Hashimoto *et al.* already mentioned that the superconducting gap in overdoped $\text{SrFe}_2(\text{As}_{0.6}\text{P}_{0.4})_2$ and $\text{BaFe}_2(\text{As}_{0.36}\text{P}_{0.64})_2$ has nodes [22]. Therefore, our observation of significant κ_0/T in the underdoped regime, particularly in the heavily underdoped $\text{BaFe}_2(\text{As}_{0.82}\text{P}_{0.18})_2$, further shows the robustness of nodal superconductivity against doping in P- and Ru-doped 122 iron pnictides.

The field dependence of κ_0/T can provide further support for the gap nodes [33]. In Fig. 4, the normalized $(\kappa_0(T)/\kappa_{N0}(T))$ of OP20K, UD17K, and UD4K are plotted as a function of H/H_{c2} . For UD4K, κ/T saturates above $H = 3 \text{ T}$, as seen in Fig. 3(c), which is determined as its bulk H_{c2} . For OP20K and UD17K, we use their H_{c2} estimated from resistivity measurements. To choose a slightly different bulk H_{c2} does not affect our discussion on the field dependence of κ_0/T . Similar data of an overdoped *d*-wave cuprate superconductor Tl-2201 [34], and $\text{BaFe}_2(\text{As}_{0.67}\text{P}_{0.33})_2$ [16] are also plotted for comparison.

For a nodal superconductor such as Tl-2201 in magnetic field, delocalized states exist out the vortex cores and dominate the heat transport in the vortex state, in contrast to the *s*-wave superconductor. At low field, the Doppler shift due to superfluid flow around the vortices will yield an $H^{1/2}$ growth in quasiparticle density of states (the Volovik effect [35]), thus the $H^{1/2}$ field dependence of κ_0/T . From Fig. 4, the behavior of $\kappa_0(H)/T$ in OP20K, UD17K, and UD4K clearly mimics that in Tl-2201 and $\text{BaFe}_2(\text{As}_{0.67}\text{P}_{0.33})_2$. In the inset of Fig. 4, the $\kappa_0(H)/T$ of OP20K, UD17K, and UD4K obey the $H^{1/2}$ dependence at low field, which supports the existence of gap nodes.

To our knowledge, so far there are five iron-based superconductors displaying nodal superconductivity, including KFe_2As_2 [10, 11], underdoped $\text{Ba}_{1-x}\text{K}_x\text{Fe}_2\text{As}_2$ ($x < 0.16$) [14], $\text{BaFe}_2(\text{As}_{1-x}\text{P}_x)_2$ [15, 16], LaFePO [19–

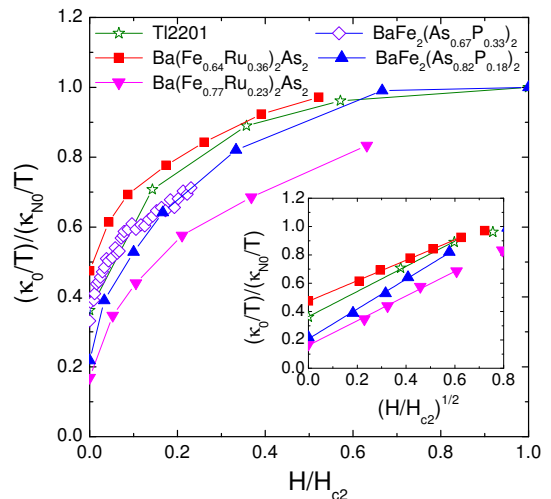


FIG. 4: (Color online). Normalized residual linear term κ_0/T of $\text{Ba}(\text{Fe}_{0.64}\text{Ru}_{0.36})_2\text{As}_2$, $\text{Ba}(\text{Fe}_{0.77}\text{Ru}_{0.23})_2\text{As}_2$, and $\text{BaFe}_2(\text{As}_{0.82}\text{P}_{0.18})_2$ as a function of H/H_{c2} . Similar data of an overdoped *d*-wave cuprate superconductor Tl-2201 [34], and $\text{BaFe}_2(\text{As}_{0.67}\text{P}_{0.33})_2$ [16] are also shown for comparison. The behaviors of $\kappa_0(H)/T$ in OP20K, UD17K, and UD4K clearly mimic that in Tl-2201 and $\text{BaFe}_2(\text{As}_{0.67}\text{P}_{0.33})_2$. Inset: the same data of OP20K, UD17K, UD4K, and Tl-2201 plotted against $(H/H_{c2})^{1/2}$. The lines represent the $H^{1/2}$ dependence.

21], and LiFeP [22]. Here we only consider the “in-plane nodes”, not counting the “*c*-axis nodes” in underdoped and overdoped $\text{Ba}(\text{Fe}_{1-x}\text{Co}_x)_2\text{As}_2$ as suggested by *c*-axis heat transport experiments [36]. For the extremely hole-doped KFe_2As_2 , the nodal gap may have *d*-wave symmetry, and result from the direct intra-pocket interaction via antiferromagnetic fluctuations, due to the lack of electron pockets [10, 37, 38]. For underdoped $\text{Ba}_{1-x}\text{K}_x\text{Fe}_2\text{As}_2$, it is still not clear how the superconducting gap transforms from nodeless to nodal at $x \approx 0.16$ [14]. The rest three compounds, $\text{BaFe}_2(\text{As}_{1-x}\text{P}_x)_2$, LaFePO , and LiFeP , have stimulated various interpretations of the effect of isovalent P doping [23–26], and may represent a peculiar superconducting mechanism.

Our new finding of nodal superconductivity in $\text{Ba}(\text{Fe}_{1-x}\text{Ru}_x)_2\text{As}_2$ reveals the similarity between the isovalently Ru- and P-doped iron pnictides. In this sense, the P doping is not that special for inducing nodal superconductivity now, and the puzzle of P doping in iron-based superconductors has been partially unwrapped. What next one needs to do is to find out the common origin for the nodal superconductivity in these isovalently doped iron pnictides.

Due to the smaller size of P ion than As ion, one common structural feature of the P-doped compounds is the decrease of pnictogen height h_{Pn} and increase of As-Fe-As angle [32, 39, 40]. The substitution of larger Ru ion for Fe ion in $\text{Ba}(\text{Fe}_{1-x}\text{Ru}_x)_2\text{As}_2$ results in the increase of *a* lattice parameter and decrease of *c* lattice param-

eter, thus the decrease of pnictogen height and increase of As-Fe-As angle [28]. Therefore, both the P and Ru dopants cause the same trend of structure change in iron arsenides.

With such structure change, the Fermi surface (FS) evolution upon isovalent P and Ru doping is rather delicate. The main feature, hole pockets around Brillouin zone (BZ) center and electron pockets around BZ corners, remains in LaFePO [41], $\text{BaFe}_2(\text{As}_{1-x}\text{P}_x)_2$ [17, 18, 31], $\text{Ba}(\text{Fe}_{1-x}\text{Ru}_x)_2\text{As}_2$ [42, 43], and LiFeP [44]. For LaFePO, Kuroki *et al.* have attributed the low- T_c nodal pairing to the lack of Fermi surface γ around (π, π) in the unfolded Brillouin zone, due to the low pnictogen height [23]. For $\text{BaFe}_2(\text{As}_{1-x}\text{P}_x)_2$, Suzuki *et al.* have proposed three-dimensional nodal structure in the largely warped hole Fermi surface and no nodes on the electron Fermi surface [26]. This is supported by recent ARPES experiments, which found nodal gap in the expanded α hole pocket at $k_z = \pi$ in $\text{BaFe}_2(\text{As}_{0.7}\text{P}_{0.3})_2$ [18], however, it conflicts with earlier ARPES results which have constrained the nodes on the electron pockets [17]. Since ARPES experiments did not find significant changes in the shape of the Fermi surface or in the Fermi velocity over a wide range of doping levels in $\text{Ba}(\text{Fe}_{1-x}\text{Ru}_x)_2\text{As}_2$, Dhaka *et al.* speculated that its superconducting mechanism relies on magnetic dilution which leads to the reduction of the effective Stoner enhancement [43]. In LiFeP, the middle hole pocket has significantly lower mass enhancement than the other pockets, which implies that the electron-hole scatter rate is suppressed for this pocket and may result in the lower T_c and nodal gap [44].

While the clues for nodal superconductivity are not very clear from the FS topology except for KFe_2As_2 , Hashimoto *et al.* gathered the available data for the low-energy quasiparticle excitations in several iron-pnictide superconductors, and suggested that there is a threshold value of $h_{P_n} \sim 1.33$ Å, below which all the superconductors exhibit nodal superconducting state [22]. If this is the case, there may exist a transition from nodal to nodeless state tuned by h_{P_n} in underdoped $\text{Ba}(\text{Fe}_{1-x}\text{Ru}_x)_2\text{As}_2$ and $\text{BaFe}_2(\text{As}_{1-x}\text{P}_x)_2$. To test this idea, we estimate $h_{P_n} = 1.317, 1.333, 1.340$ Å for OP20K, UD17K, UD4K from the roughly linear increase of h_{P_n} with decreasing Ru or P doping [28, 32].

One can see that both h_{P_n} of UD17K and UD4K are slightly larger than the proposed threshold value 1.33 Å. In particular, the h_{P_n} of UD4K is comparable to that of overdoped $\text{Ba}(\text{Fe}_{0.89}\text{Co}_{0.11})_2\text{As}_2$, which is a nodeless superconductor [22]. Since our thermal conductivity data suggest UD17K and UD4K are nodal superconductors, h_{P_n} should not be considered as the only parameter for tuning between nodeless and nodal superconducting states. By saying this, we do not deny its importance, since h_{P_n} of the underdoped $\text{Ba}(\text{Fe}_{1-x}\text{Ru}_x)_2\text{As}_2$ and $\text{BaFe}_2(\text{As}_{1-x}\text{P}_x)_2$ are still very close to the threshold value 1.33 Å. More careful considerations of the struc-

tural parameters, FS topology, and local interactions are needed to clarify the origin of the nodal superconductivity in isovalently doped iron pnictides.

In summary, we have measured the thermal conductivity of $\text{Ba}(\text{Fe}_{0.64}\text{Ru}_{0.36})_2\text{As}_2$, $\text{Ba}(\text{Fe}_{0.77}\text{Ru}_{0.23})_2\text{As}_2$, and $\text{BaFe}_2(\text{As}_{0.82}\text{P}_{0.18})_2$ single crystals down to 50 mK. A significant κ_0/T at zero field and an $H^{1/2}$ field dependence of $\kappa_0(H)/T$ at low field give strong evidences for nodal superconductivity in all three compounds. Comparing with previous P-doped iron pnictides, our new finding suggests that the nodal superconductivity induced by isovalent Ru and P doping may have the same origin. With decreasing doping level, nodal superconducting state persists robustly in heavily underdoped $\text{BaFe}_2(\text{As}_{0.82}\text{P}_{0.18})_2$, suggesting that the h_{P_n} is not the only tuning parameter, thus putting constraint on theoretical models. Finding out the origin of these nodal superconducting states will be crucial for getting a complete electronic pairing mechanism in the iron-based high- T_c superconductors.

This work is supported by the Natural Science Foundation of China, the Ministry of Science and Technology of China (National Basic Research Program No: 2009CB929203 and 2012CB821402), Program for Professor of Special Appointment (Eastern Scholar) at Shanghai Institutions of Higher Learning, and STCSM of China. The work at Postech was supported by Leading Foreign Research Institute Recruitment Program(2010-00471), Basic Science Research Programs (2010-0005669) through the National Research Foundation of Korea(NRF)

* E-mail: shiyan_li@fudan.edu.cn

-
- [1] Y. Kamihara *et al.*, J. Am. Chem. Soc. **130**, 3296 (2008).
 - [2] J. Paglione and R. L. Greene, Nature Physics **6**, 645 (2010).
 - [3] Fa Wang and Dung-hai Lee, Science **332**, 200 (2011).
 - [4] P. J. Hirschfeld, M. M. Korshunov, and I. I. Mazin, Rep. Prog. Phys. **74**, 124508 (2011), and references therein.
 - [5] H. Ding *et al.*, EPL **83**, 47001 (2008).
 - [6] K. Terashima *et al.*, Proc. Natl. Acad. Sci. **106**, 7330 (2009).
 - [7] X. G. Luo *et al.*, Phys. Rev. B **80**, 140503(R) (2009).
 - [8] L. Ding *et al.*, New J. Phys. **11**, 093018 (2009).
 - [9] M. A. Tanatar *et al.*, Phys. Rev. Lett. **104**, 067002 (2010).
 - [10] J. K. Dong *et al.*, Phys. Rev. Lett. **104**, 087005 (2010).
 - [11] K. Hashimoto *et al.*, Phys. Rev. B **82**, 014526 (2010).
 - [12] J. K. Dong *et al.*, Phys. Rev. B **81**, 094520 (2010).
 - [13] Yunkyu Bang, Phys. Rev. Lett. **104**, 217001 (2010).
 - [14] J.-Ph. Reid *et al.*, arXiv:1105.2232.
 - [15] Y. Nakai *et al.*, Phys. Rev. B **81**, 020503(R) (2010).
 - [16] K. Hashimoto *et al.*, Phys. Rev. B **81**, 220501(R) (2010).
 - [17] T. Shimojima *et al.*, Science **332**, 564 (2011).
 - [18] Y. Zhang *et al.*, arXiv:1109.0229.
 - [19] J. D. Fletcher *et al.*, Phys. Rev. Lett. **102**, 147001 (2009).

- [20] C. W. Hicks *et al.*, Phys. Rev. Lett. **103**, 127003 (2009).
- [21] M. Yamashida *et al.*, Phys. Rev. B **80**, 220509 (2009).
- [22] K. Hashimoto *et al.*, arXiv:1107.4505, Phys. Rev. Lett. in press.
- [23] K. Kuroki *et al.*, Phys. Rev. B **79**, 224511 (2009).
- [24] F. Wang, H. Zhai, and D.-H. Lee, Phys. Rev. B **81**, 184512 (2010).
- [25] R. Thomale *et al.*, Phys. Rev. Lett. **106**, 187003 (2011).
- [26] K. Suzuki, H. Usui, and K. Kuroki, J. Phys. Soc. Jpn. **80**, 013710 (2011).
- [27] S. Sharma *et al.*, Phys. Rev. B **81**, 174512 (2010).
- [28] F. Rullier-Albenque *et al.*, Phys. Rev. B **81**, 224503 (2010).
- [29] A. Thaler *et al.*, Phys. Rev. B **82**, 014534 (2010).
- [30] M. J. Eom, S. W. Na, C. Hoch, R. K. Kremer, J. S. Kim, arXiv:1105.2232.
- [31] Z. R. Ye *et al.*, arXiv:1105.5242.
- [32] S. Kasahara *et al.*, Phys. Rev. B **81**, 184519 (2010).
- [33] H. Shakeripour *et al.*, New J. Phys. **11**, 055065 (2009).
- [34] C. Proust *et al.*, Phys. Rev. Lett. **89**, 147003 (2002).
- [35] G. E. Volovik, JETP Lett. **58**, 469 (1993).
- [36] J.-Ph. Reid *et al.*, Phys. Rev. B **82**, 064501 (2010).
- [37] R. Thomale *et al.*, Phys. Rev. Lett. **107**, 117001 (2011).
- [38] S. Maiti *et al.*, Phys. Rev. Lett. **107**, 147002 (2011).
- [39] M. Tegel *et al.*, arXiv:0805.1208, Z. Naturforsch. B - Chem. Sci. **63**, 1057 (2008).
- [40] S. Jiang *et al.*, J. Phys. Condens. Matter **21**, 382203 (2009).
- [41] D. H. Lu *et al.*, Nature (London) **455**, 81 (2008).
- [42] V. Brouet *et al.*, Phys. Rev. Lett. **105**, 087001 (2010).
- [43] R. S. Dhaka *et al.*, arXiv:1108.0711, Phys. Rev. Lett. in press.
- [44] C. Putzke *et al.*, arXiv:1107.4375.